Muscle Synergy Analysis of Human Standing-up Motion Using Forward Dynamic Simulation with Four Body Segment Model

Qi An, Yuki Ishikawa, Tetsuro Funato, Shinya Aoi, Hiroyuki Oka, Hiroshi Yamakawa, Atsushi Yamashita, and Hajime Asama

Abstract Human motor behavior can be generated using distributed system. In this study, human standing-up motion is focused as an important daily activity. Especially, 13 muscle activation of lower body and trunk during human standing-up motion is decomposed into small numbers of modules of synchronized muscle activation called muscle synergy. Moreover human musculoskeletal model is developed with four rigid body segment based on dynamics and anatomical characteristics of human body. Forward dynamic simulation with the developed model showed that four muscle synergies had their own contribution toward body function: bending forward, moving the center of mass forward, extending whole body, and decelerating the center of mass. Results also indicated that combinations of four modules of synchronized muscle activation could generate human standing-up motion rather than controlling individual muscles.

1 Introduction

In this study, we analyze the human motion in terms of distributed modules of synchronized muscle activation called muscle synergy. When humans move, they need to incorporate with their redundant body system, i.e. humans have to control larger degrees of freedom of muscles than that of joints in order to achieve the targeted kinematics. Therefore, muscle activation cannot be determined although the target kinematics is given. To solve this ill-posed problem, the concept of muscle synergy

Qi An, Yuki Ishikawa, Hiroyuki Oka, Hiroshi Yamakawa, Atsushi Yamashita, and Hajime Asama
The University of Tokyo, 3-7-1 Hongo, Bunkyou-ku, Tokyo, Japan, 1138656
e-mail: anqi@robot.t.u-tokyo.ac.jp

Tetsuro Funato
The University of Electro-Communications, 1-5-1 Chofugaoka, Chofu, Tokyo Japan, 1828585

Shinya Aoi
Kyoto University, Kyoto Daigaku Katsura, Nishikyo-ku, Kyoto, Japan, 6158540

was previously proposed by Bernstein [1]. It suggested that humans did not control their individual muscles, but they autonomously coordinated muscle synergies. Regarding the analysis of muscle synergy, it has been suggested that five modules of synchronized muscle activation can account for a large amount of human locomotion [2]. Another study demonstrated that some basic behavior of a frog movement could be explained with small sets of synergies [3].

In our previous study, we analyzed human standing-up motion as an important daily activity. Previously, we developed the musculoskeletal model to ensure that three muscle synergies were corresponded to three kinematic movement of human standing-up motion [4]. Moreover forward dynamic simulation validated that three muscle synergies could generate human standing-up motion. However, our previous study considered only the muscles in lower body and it could not explain one of the four important phases of the standing-up motion, which was forward bending of trunk. In order to fully understand and express human standing-up motion with muscle synergies, it is necessary to extract important modules from both lower body and upper trunk.

Therefore, in this study, our objectives are to elucidate important muscle synergies from muscle activation of both lower body and trunk of human standing-up motion. Moreover, musculoskeletal model is developed to represent human body and muscles of lower body and trunk to clarify that human standing-up motion can be achieved by four muscle synergies.

2 Methods

2.1 Synergy Model

This paper has employed the muscle synergy model to represent muscle activation of human movement. It assumes that muscle activation during human movement can be decomposed into spatial structure and temporal structure. Spatial structure is defined as muscle synergy, and it determines relative excitation level of muscles. On the other hand, temporal structure is defined as weighting coefficient which determines time-varying amplitudes of muscle synergies. This muscle synergy model is expressed as in eq. (1).

$$\mathbf{M} \cong \mathbf{WC}, \tag{1}$$

where $\mathbf{M}$ is a matrix to express muscle activation, $\mathbf{W}$ represents muscle synergy matrix, and $\mathbf{C}$ represents weighting coefficient matrix. Muscle activation matrix $\mathbf{M}$ consists of muscle activation vector $\mathbf{m}_i$ to indicate discrete time-varying muscle activation for different n muscles. Its element $m_i(t)$ indicates muscle activation level of i-th muscle ($i = 1 \cdots n$) at time t ($1 \leq t \leq T_{\max}$) as shown in eq. (2). Muscle synergy matrix $\mathbf{W}$ consists of muscle synergy vector $\mathbf{w}_j$ to represent j-th muscle synergy ($j = 1 \cdots N$) as in eq. (3). Elements of the muscle vector $\mathbf{w}_j$ is w_{ij} to indicate activation level of i-th muscle in j-th muscle synergy. Time-varying weighting coefficient matrix $\mathbf{C}$ consists of the vector $\mathbf{c}_j$, and its component $c_j(t)$ indicates weighting coefficient of j-th synergy at time t as in eq. (4).

$$\mathbf{M} = \begin{pmatrix} \mathbf{m}_1(t) \\ \mathbf{m}_2(t) \\ \vdots \\ \mathbf{m}_n(t) \end{pmatrix} = \begin{pmatrix} m_1(1) & \cdots & m_1(T_{\max}) \\ \vdots & \ddots & \vdots \\ m_n(1) & \cdots & m_n(T_{\max}) \end{pmatrix}, \tag{2}$$

$$\mathbf{W} = (\mathbf{w}_1 \cdots \mathbf{w}_N) = \begin{pmatrix} w_{11} & \cdots & w_{1N} \\ \vdots & \ddots & \vdots \\ w_{n1} & \cdots & w_{nN} \end{pmatrix}, \tag{3}$$

$$\mathbf{C} = \begin{pmatrix} \mathbf{c}_1(t) \\ \mathbf{c}_2(t) \\ \vdots \\ \mathbf{c}_N(t) \end{pmatrix} = \begin{pmatrix} c_1(1) & \cdots & c_1(T_{\max}) \\ \vdots & \ddots & \vdots \\ c_N(1) & \cdots & c_N(T_{\max}) \end{pmatrix}. \tag{4}$$

Figure 1 shows a schematic design of muscle synergy model. In the figure, three muscle synergies represent muscle activation. Figure 1 (a) indicates three muscle synergies ($\mathbf{w}_{1,2,3}$) and the bars in each square show excitation level of n muscles involved in j-th muscle synergy. On the other hand, Fig. 1 (b) shows corresponded weighting coefficients ($\mathbf{c}_{1,2,3}(t)$). In Fig. 1 (c), n muscle activations are expressed by linear summation of three muscle synergies and their weighting coefficients. In order to decide muscle synergy matrix $\mathbf{W}$ and its time-varying weighting coefficients $\mathbf{C}$, non-negative matrix factorization (NNMF) [5] is used.

It is necessary to decide the best number of muscle synergies to represent human standing-up motion. Coefficient of determination R^2 is used to evaluate how much variance of observed muscle activations can be explained from muscle synergies. The number of muscle synergies is decided from two criteria. The first criterion is

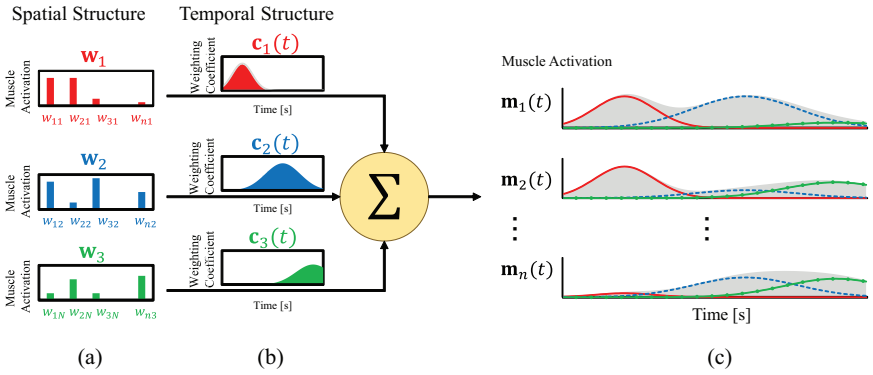

Fig. 1 Muscle Synergy Model. (a) muscle synergy determines relative excitation level of each muscle. (b) shows time-varying weighting coefficients corresponded to synergies. (c) shows muscle activations. Red solid lines, blue dashed lines, and green solid lines with circle markers show muscle activation generated from each muscle synergy and corresponded time-varying weighting coefficients. It indicates that three muscle synergies and their weighting coefficients generate n muscle activations.

that muscle synergies can account for a large amount ($> 95\%$) of total variance of muscle activation [6]. The other criterion is how the additional synergy affects the performance of muscle synergy to explain the variance of muscle activation. One-factor analysis of variance (ANOVA) is used to assess the effect of the number of muscle synergies on the accuracy of the model. If there is a statistical significance, the post-hoc test (Tukey-Kramer test) is used to evaluate the effect of increase in the number of muscle synergies. Statistical significance level p is set to 0.05.

2.2 Musculoskeletal Model

This study focuses on sagittal movement of standing-up motion, and the human body is modelled by four segments of shank, thigh, pelvis, and HAT (head, arm and trunk). Figure 2 (a) illustrates the developed skeletal model. Joint angles $\theta_{k(k=1,2,3,4)}$ are defined as the angle from the distal segment. Segment length, position of center of mass, mass, moment of inertia are defined as L_k, L_k^{G}, M_k, and I_k. Given these parameters, equation of motion is expressed as in eq. (5).

$$\mathbf{I}(\Theta,\dot{\Theta})\ddot{\Theta}+\mathbf{h}(\Theta,\dot{\Theta})+\mathbf{g}(\Theta) = \mathbf{T}_{\mathrm{JNT}}+\Phi(\Theta,\dot{\Theta}), \tag{5}$$

$$\mathbf{T}_{\mathrm{JNT}} = \mathbf{T}_{\mathrm{MUS}}+\mathbf{T}_{\mathrm{POS}}, \tag{6}$$

where $\mathbf{I}(\Theta,\dot{\Theta}) \in \mathbb{R}^{4\times4}$, $\mathbf{h}(\Theta,\dot{\Theta}) \in \mathbb{R}^{4\times1}$, $\mathbf{g}(\Theta) \in \mathbb{R}^{4\times1}$ indicate inertia matrix, non-linear term, and gravitational force term. They are obtained from Lagrange equation. $\Theta \in \mathbb{R}^{4\times1}$ indicates a matrix to represent joint angles. Component of Θ is each joint angle θ_k. $\Phi(\Theta,\dot{\Theta}) \in \mathbb{R}^{4\times1}$ indicates horizontal and vertical reaction force generated from elastic and viscous elements as shown in Fig. 2 (b). Reaction force is applied to the hip joint when the hip position is lower than the chair height H. $\mathbf{T}_{\mathrm{JNT}} \in \mathbb{R}^{4\times1}$ indicates joint torque, and it consists of muscular torque ($\mathbf{T}_{\mathrm{MUS}}$) and posture stabilization torque ($\mathbf{T}_{\mathrm{POS}}$) as in eq. (6). $\mathbf{T}_{\mathrm{MUS}}$ is determined from the muscle model as explained below. $\mathbf{T}_{\mathrm{POS}}$ is the torque to stabilize posture, and it is determined from PID control to follow the desired trajectories.

Thirteen muscles in lower body and trunk which either flex or extend the body segments are considered including mono and bi articular muscles (Fig. 2 (c)): tibialis anterior (TA), gastrocenomius (GAS), soleus (SOL), rectus femoris (RF), vastus lateralis (VAS), biceps femoris long head (BFL), biceps femoris short head (BFS), gluteus maximus (GMA), sartorius (SAR), rectus abdominis (RA), elector spine (ES), latissimus dorsi (LD), and iliopsoas (IL).

$\mathbf{T}_{\mathrm{MUS}}$ is generated from individual muscles and it is calculated from moment arm of muscles and muscular tension as in eq. (7). Moment arm matrix $\mathbf{A} \in \mathbb{R}^{4\times n}$ indicates the moment arm length of muscles to joints (eq. (8)). Its component r_{ki} indicates the moment arm length of i-th muscle on the joint k. Moment arm length r_{ki} is zero if the muscle i does not attach the joint k, and otherwise it is either positive or negative depending on how the muscle acts on the ankle, knee, hip and pelvis (extension or flexion). In this study, moment arm is supposed to be constant regardless of body posture.

$$\mathbf{T}_{\mathrm{MUS}} = \mathbf{AF}(l_i, \dot{l}_i, m_i), \tag{7}$$

$$\mathbf{A} = \begin{pmatrix} r_{11} & \cdots & r_{1n} \\ \vdots & \ddots & \vdots \\ r_{41} & \cdots & r_{4n} \end{pmatrix}. \tag{8}$$

$\mathbf{F} \in \mathbb{R}^{n\times 1}$ indicates the vector of muscular tension. Muscle is represented by Hill type model [7] (Fig. 2 (c)). Using the model, muscular force of i-th muscle F_i is generated from two components: contractile element (CE) and parallel elastic element (PE). The force generated by contractile element F_i^{CE} is calculated from maximum isometric force ($F_i^{\max}$), muscle activation (m_i), and muscle dynamics. When normalized muscle length $\widetilde{l_i}$ and normalized muscular velocity $\widetilde{v_i}$ are given, force-length relationship $f_{\mathrm{fl}}(\widetilde{l_i})$ and force-velocity relationship $f_{\mathrm{fv}}(\widetilde{v_i})$ are considered as muscle dynamics [8][9]. On the other hand, PE generates force when the muscle lnegth l_i is longer than its optimal length as in eq. (11). The force of PE (F_i^{PE}) is calculated according to the normalized muscle length ($\widetilde{l_i}$) [10]. The normalized muscle length $\widetilde{l_i}$ is decided from moment arm and changes of joint angle ($d\theta_k$) (eq. (12)) [11]. The optimal muscle length is equal to the muscle length when humans stand vertically. The normalized muscular velocity $\widetilde{v_i}$ is obtained from eq. (13)).

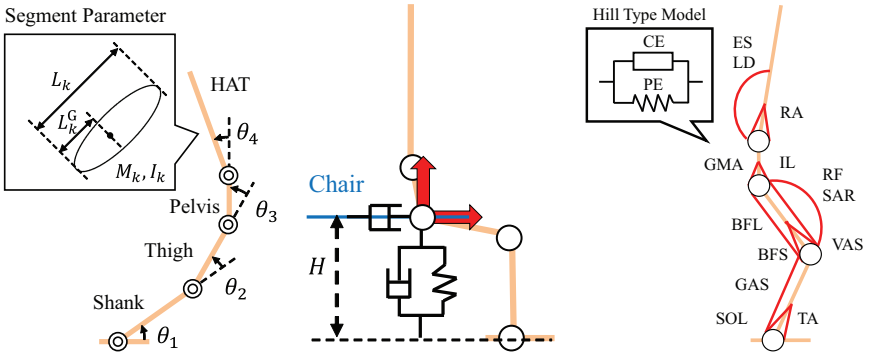

Fig. 2 Developed Musculoskeletal Model. (a) shows four segment model of human body: shank, thigh, pelvis, and HAT. (b) shows the floor model which applies horizontal and vertical forces on the hip joint with viscous and kinetic elements. (c) shows considered 13 muscles. Hill type model is used to represent muscles.

$$F_i(l_i, \dot{l}_i, m_i) = F_i^{\mathrm{CE}} + F_i^{\mathrm{PE}}, \tag{9}$$

$$F_i^{\mathrm{CE}} = F_i^{\max} f_{\mathrm{fl}}(\widetilde{l_i}) f_{\mathrm{fv}}(\widetilde{v_i}) m_i, \tag{10}$$

$$F_i^{\mathrm{PE}} = F_i^{\max} f_{\mathrm{pe}}(\widetilde{l_i}), \tag{11}$$

$$\widetilde{l_i} = (l_i^o + \sum_{k=1}^{4} (r_{ki} d\theta_k))/l_i^o. \tag{12}$$

$$\widetilde{v_i} = \frac{1}{10 l_i^o} \frac{dl_i}{dt}. \tag{13}$$

$\mathbf{T}_{\mathrm{POS}}$ is generated from PID control to follow the target kinematics as shown in eqs. (14–16). In the equations, $\mathbf{q}(t)$ and $\dot{\mathbf{q}}(t)$ indicate the model's joint angle and angular velocity from the horizontal direction. On the other hand, $\hat{\mathbf{q}}(t)$ and $\hat{\dot{\mathbf{q}}}(t)$ are targeted kinematics. Additionally, nervous transmission delay λ is considered in this study to calculate $\mathbf{T}_{\mathrm{POS}}$. Gains for proportional, integral and derivative control are manually determined by trying and error.

$$\mathbf{T}^{\mathrm{Pos}}(t) = \begin{cases} 0.0 & \text{when } t < \lambda_{\mathrm{delay}} \\ \mathbf{K}_{\mathrm{P}}^q \Delta\mathbf{q}(t-\lambda) + \mathbf{K}_{\mathrm{I}}^q \int_{t-T_{\mathrm{i}}}^{t} \Delta\mathbf{q}(\psi-\lambda) d\psi + \mathbf{K}_{\mathrm{D}}^q d\Delta\mathbf{q}(t-\lambda) & \\ \quad + \mathbf{K}_{\mathrm{P}}^q \Delta\dot{\mathbf{q}}(t-\lambda) + \mathbf{K}_{\mathrm{I}}^q \int_{t-T_{\mathrm{i}}}^{t} \Delta\dot{\mathbf{q}}(\psi-\lambda) d\psi + \mathbf{K}_{\mathrm{D}}^q d\Delta\dot{\mathbf{q}}(t-\lambda) & \\ & \text{when } t \geq \lambda_{\mathrm{delay}} \end{cases} \tag{14}$$

$$\Delta\mathbf{q}(t) = \hat{\mathbf{q}}(t) - \mathbf{q}(t) \tag{15}$$

$$\Delta\dot{\mathbf{q}}(t) = \hat{\dot{\mathbf{q}}}(t) - \dot{\mathbf{q}}(t) \tag{16}$$

2.3 Forward Dynamics Simulation

Forward dynamic simulation is conducted to generate movement with developed musculoskeletal model. Before the simulation, body kinematics, reaction force, and muscle activation are averaged for all data in a measurement experiment explained in the latter section. In order to generate the standing-up motion, firstly joint torque $\mathbf{T}_{\mathrm{JNT}}$ is calculated using inverse dynamics from average body kinematics and reaction force. Then the joint torque $\mathbf{T}_{\mathrm{JNT}}$ is decomposed to the muscle activation $\mathbf{m}_i'$ which can necessarily generate the joint torque for the standing-up motion. Since our musculoskeletal model has bi-articular muscles, the muscle activation cannot be determined exclusively from the given joint torque. Therefore in this study, the muscle activation $\mathbf{m}_i'$ is decided thorough optimization methodology to minimize squared error between muscle activation $\mathbf{m}_i'$ and measured muscle activation $\mathbf{m}_i$.

Muscle synergy $\mathbf{w}_j'$ and time-varying weighting coefficient $\mathbf{c}_j'$ are calculated from muscle activation $\mathbf{m}'$ to generate the standing-up motion. In particular, time-varying weighting coefficient is expressed in trapezoid wave. During the simulation $\mathbf{T}_{\mathrm{JNT}}$ consists of muscular torque $\mathbf{T}_{\mathrm{MUS}}$ and posture stabilization torque $\mathbf{T}_{\mathrm{POS}}$. Muscular torque is generated from $\mathbf{w}_j'$ and $\mathbf{c}_j'$ and body posture Θ and $\dot{\Theta}$. Posture stabilization

torque ($\mathbf{T}_{POS}$) is decided to follow the average body kinematics. The average joint angles and angular velocities at the start of the data are used for initial posture of the simulation. Segment parameters are decided from measured data. For numerical calculation, fourth order Runge-Kutta method is used with time step of 1 ms.

2.4 Analysis of Standing-up Motion

In order to investigate the relationship between muscle synergies and body kinematics, four kinematic important phases are focused. It is known that there are four characteristic events (phases 1–4) in human standing-up motion as following [12].

1. Phase 1: Bends trunk forward to generate momentum.
2. Phase 2: Rises hip to move center of mass forward.
3. Phase 3: Extends body to move center of mass upward.
4. Phase 4: Stabilizes posture.

Figure 3 illustrates movement during four phases in standing-up motion.

The start point of each phase is determined from measured body kinematics and reaction force data. The start of phase 1 is decided when humans bend their trunk forward. Therefore it is decided as the horizontal shoulder velocity exceeds the threshold p_1. Phase 2 begins when humans rise their hip, and the start time is obtained from the time when reaction force of hip is below the threshold p_2. Phase 3 starts when extension of body starts after the forward movement of center of mass. The start time of phase 3 is obtained when the horizontal knee position reaches the most front point. At last, the start point of phase 4 is obtained when humans complete the standing-up motion. It is calculated from the time when vertical shoulder velocity is below the threshold p_4. Measured data 1.0 s before and 1.0 s after the time of hip rising is used for analysis.

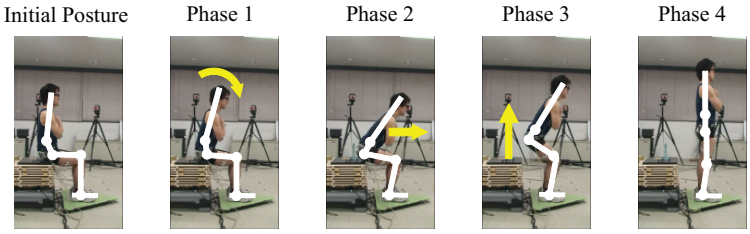

Fig. 3 Four Kinematic Phases in Standing-up Motion. In phase 1, humans start bending. In phase 2, humans move their center of mass forward. In phase 3, humans extend their body to move upward. In phase 4, humans decelerate the movement of the center of mass.

2.5 Empirical Experiment with Humans

Measurement experiment was conducted to evaluate the results of forward dynamic simulation. One young healthy male participated in the experiment (age: 27 years, height: 1.76 m, weight: 77 kg). Muscle activation was measured in 1,000 Hz by DL-720 (S&ME Corp.). In the experiment, 17 body positions were measured according to Helen Hayes marker set, and they were obtained in 200 Hz using an optical motion capture system MAC3D (MotionAnalysis Corp.). Reaction force from participants' hip and feet was measured in 64 Hz using force sensors (Nitta Corp.). Consent was obtained before starting the experiment, and this study was conducted with approval by the Institute Review Board (IRB) of the University of Tokyo.

Muscle activation data was filtered with 10 Hz high pass and 200 Hz low pass second order butterworth filter. Also muscle activation data was rectified and normalized based on maximum voluntary contraction (MVC). Body position and reaction force data were filtered with low-pass second order butterworth filter with cut-off frequency 10 Hz and 20 Hz respectively. Joint angles $\theta_{1,2,3,4}$ were calculated using SIMM (MusculoGraphics Corp.).

Our experiment consisted of two trials. Each trial continued for 150 s and the participant was asked to repeat the sit-to-stand and stand-to-sit motion during the trial. The chair height was adjusted to the knee height. During standing-up motion, the participant was asked to cross their arms in front of their chest in order to avoid the use of their hands and arms. Ankle joint angle was set vertically to the ground at the start of the motion, and the participant was told not to move their feet during measurement. Moreover, the subject was asked to perform the standing-up motion in a comfortable speed.

3 Results

3.1 Results of Measured Standing-up Motion

From the measurement experiment, 28 trials of standing-up motion were obtained. Thresholds to decide the phase start were set to 0.2 m/s, 5 N, and 0.0 m/s respectively for p1, p2, p4. In all obtained trials, average and standard deviation of start times of four phases were 0.29±0.07 s, 1.00 s, 1.42±0.10 s, and 1.70±0.25 s respectively for phases 1–4.

3.2 Results of Muscle Synergy from Measured Data

Figure 4 shows the average and standard deviation of coefficient of determination R^2 for different numbers of muscle synergies. Muscle synergies $\mathbf{w}'_j$ and time-varying

weighting coefficient $\mathbf{c}'_j$ were calculated from $\mathbf{m}'$. Coefficients of determination exceed 95% of the variance when the number of muscle synergies was four. Moreover, ANOVA revealed a statistical significance on the coefficient of determination according to the number of muscle synergies. Therefore post-hoc test was applied to the neighbouring number of synergies to investigate whether additional synergies could increase the coefficient of determination. Results showed a statistical significance between the number of muscle synergies one and two, two and three, and three and four. Therefore, the number of muscle synergies was set to be four.

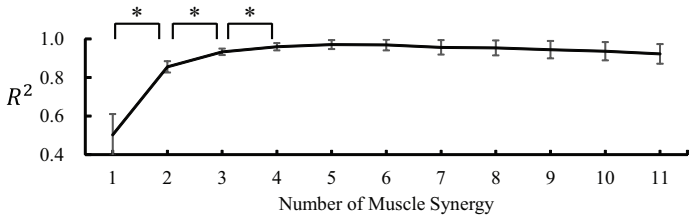

Fig. 4 Results of Coefficient of Determination. Results of statistical analysis shows that there were statistical significance between the number of muscle synergies one and two, two and three, and three and four. Moreover, four muscle synergies could explain more than 95% of muscle activation.

Figures 5 (a), (c), (e) and (g) illustrate muscle activation level included in extracted muscle synergies 1–4. Figure 5 (b), (d), (f), and (h) illustrate time-varying weighting coefficients corresponded to four different synergies. In the figures, vertical lines respectively show start time of phases 1–4.

3.3 Results of Forward Dynamics Simulation

Table 1 shows detailed segment parameters and parameters of postural control used for forward dynamic simulation. Also, coefficient of elastic elements of reaction force was 10,000 N/m for the vertical direction. Coefficients of viscous elements were set to be 300 and 400 Ns/m for horizontal and vertical directions. The chair height H was set to be 0.555 m. Nervous transmission delay was set to be 100 ms. Other parameters for muscle models were determined from previous studies [11][13][14].

Figures 6 (a)–(d) show comparison between simulated joint angles and measured joint angles of ankle, knee, hip, and lumbar respectively. Figures 6 (e)–(f) shows comparison between simulated and measured reaction force in horizontal and vertical directions. Figure 6 (g) shows movement of musculoskeletal model performing standing-up motion which is calculated from forward dynamic simulation.

Table 1 Parameters for Skeletal Model and Postural Control. Below shows parameters of skeletal model and for PID controller of foot, knee, hip and lumbar joints.

	L_K [m]	M_K [m]	L_K^G [m]	I_K [m]	$\mathbf{K}_P^\Theta$	$\mathbf{K}_I^\Theta$	$\mathbf{K}_D^\Theta$	$\mathbf{K}_P^\Theta$	$\mathbf{K}_I^\Theta$	$\mathbf{K}_D^\Theta$
Foot	0.5	4.8	0.15	0.04	250	0.15	3500	30	0	1500
Knee	0.4	9.6	0.16	0.13	350	0.15	3500	40	0	1000
Hip	0.1	17.6	0.01	0.05	80	0	1000	40	0	2500
Lumbar	0.7	48.0	0.14	3.55	400	0	1000	40	0	2500

4 Discussion

Four muscle synergies were obtained from the standing-up motion. Muscle excitation level of muscle synergies and time-varying weighting coefficients showed that

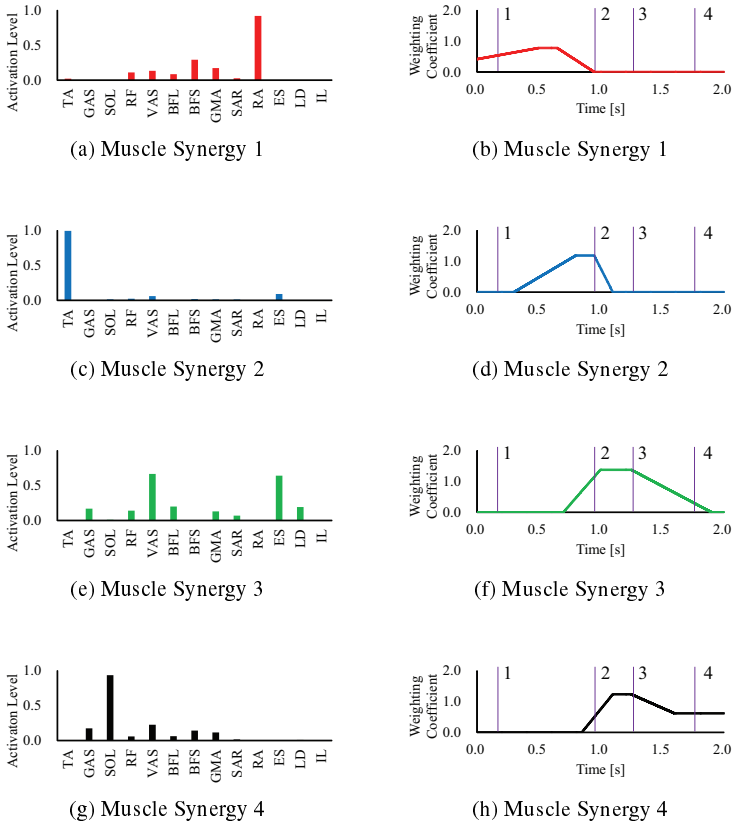

(a) Muscle Synergy 1 (b) Muscle Synergy 1

(c) Muscle Synergy 2 (d) Muscle Synergy 2

(e) Muscle Synergy 3 (f) Muscle Synergy 3

(g) Muscle Synergy 4 (h) Muscle Synergy 4

Fig. 5 Muscle Synergy of Forward Dynamics Simulation. (a), (c), (e), and (g) show relative excitation muscle activation included in each synergy. (b), (d), (f), and (h) show time-varying weighting coefficients of muscle synergies. The vertical lines show start time of four different phases.

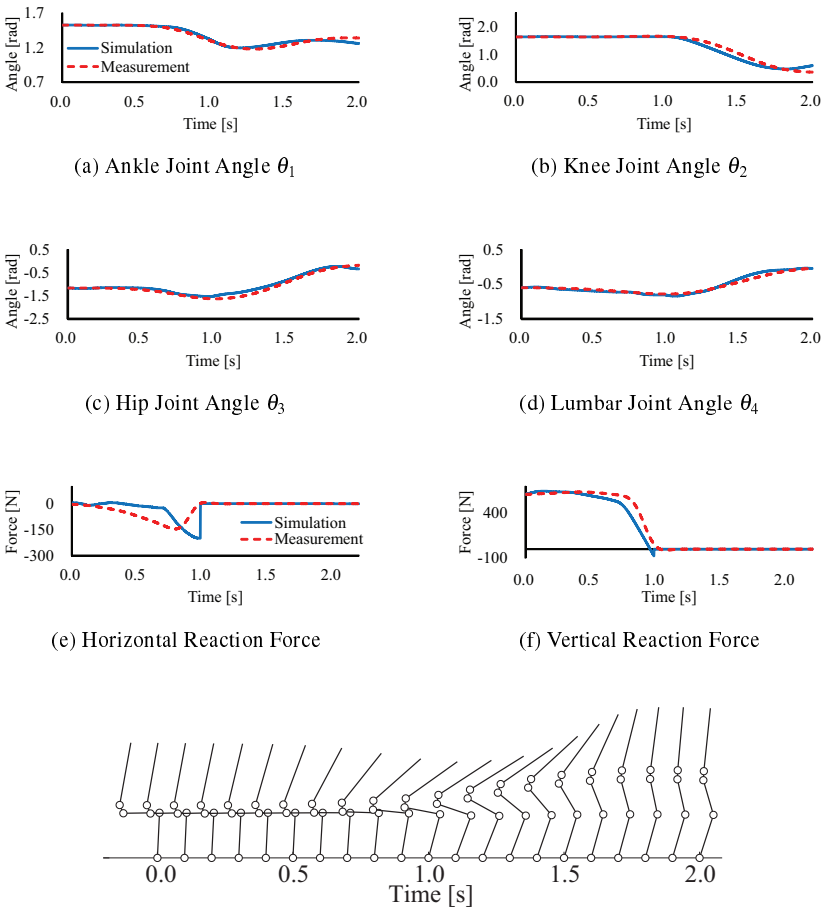

Fig. 6 Forward Dynamics Simulation Results. (a)–(d) show comparison of joint angles (θ_1–θ_4) between simulated ones (solid lines) and measured ones (dashed liens). (e)–(f) show comparison of reaction force between simulated ones (solid lines) and measured ones (dashed liens). (g) shows stick pictures of standing-up motion performing the standing-up motion.

each synergy had different contribution to human standing-up motion and it corresponded to characteristic phase of standing-up motion reported previously [12].

Muscle synergy 1 involved muscle activation of RA and it was mainly activated during phase 1. This implied that humans activated RA to flex their trunk for forward bending (generating momentum). Similarly, muscle synergy 2 was activated the most at the start time of phase 2. In muscle synergy 2, TA was mostly activated. It corresponded to the movement during phase 2 to move the center of mass forward

by dorsiflexion of the ankle (TA). On the other hand, VAS and ES were activated during muscle synergy 3 to extend their knee and trunk. This muscle synergy was mainly activated during phase 3 to extend whole body and lift up the center of mass upward. At last, activation of muscle synergy 4 was mainly seen in phase 4. In the synergy 4, SOL was activated to extend ankle joint to decelerate the horizontal movement of center of mass.

Compared to our previous study [4], four muscle synergies have been extracted from human standing-up motion instead of three muscle synergies. Since our previous study only considered lower body muscles, it could not fully express the movement of trunk. However, this study has included additional muscles in trunk, and therefore the muscle synergy 1 was newly obtained. Although most of the studies to analyze standing-up motion considers only three joint angles of ankle, knee and hip, this study develops musculoskeletal model of four rigid body segments according to the anatomical attachment and contribution of each muscle on body joints. Our forward dynamics simulation results showed that four muscle synergies could achieve the standing-up motion.

5 Conclusions and Future Works

Four essential muscle synergies were extracted from muscle activation of lower body and trunk during human standing-up motion. Muscles activation level involved in each muscle synergy and its time-varying weighting coefficients correspond to characteristic body movement of standing-up motion. Moreover musculoskeletal model was developed considering dynamics and anatomical characteristics of human body. Our forward dynamics simulation showed that four muscle synergies could successfully achieve the human standing-up motion instead of controlling individual muscles.

One of our future direction will be study of how the obtained muscle synergies are robust for environmental changes. For example, it is necessary to investigate whether four muscle synergies can realize the motion from different chair seat heights or different feet positions. Another interesting direction is to analyze structure of muscle synergies. In the current study, four individual muscle synergies are obtained, but it is unclear whether each synergy works independently or one synergy is dependent on another. Using the developed musculoskeletal model, relationship between each muscle synergy will be studied.

Acknowledgements This work was in part supported by JSPS KAKENHI Grant Number 26120005 and 26120006, the MEXT KAKENHI, Gtant-in-Aid for Scientific Research (B) 24300198, JST RISTEX Service Science, Solutions and Foundation Integrated Research Program, and Grant-in-Aid for JSPS Fellows 24·8702.

References

1. Bernstein N, "The Co-ordination and Regulation of Movement", Pergamon, Oxford, 1967.
2. Ivanenko YP, Poppele RE, and Lacquaniti F, "Five Basic Muscle Activation Patterns Account for Muscle Activity during Human Locomotion", Journal of Physiology, vol. 556, pp. 267-282, 2004.
3. d'Avella A and Bizzi E, "Shared and Specific Muscle Synergies in Natural Motor Behavior", Proceedings of the National Academy of Sciences, vol. 102, pp. 3076-3081, 2005.
4. An Q, Ishikawa Y, Funato T, Aoi S, Oka H, Yamakawa H, Yamashita A and Asama H: "Generation of Human Standing-up Motion with Muscle Synergies Using Forward Dynamic Simulation", Proceedings of the 2014 IEEE International Conference on Robotics and Automation (ICRA2014), pp. 730-735, Hong Kong (China), June 2014.
5. Lee DD and Seun HS, "Learning the Parts of Objects by Non-Negative Matrix Factorization", Nature, vol. 401, pp. 788-791, 1999.
6. Ting LH and Macpherson JM, "A Limited Set of Muscle Synergies for Force Control During a Postural Task", Journal of Neurophysiology, vol. 93, pp. 609-613, 2005.
7. Zajac FE, "Muscle and Tendon: Properties, Models, Scaling, and Application to Biomechanics and Motor Control", Critical Reviews in Biomedical Engineering, vol. 17, pp. 359-411, 1989.
8. Hatze H, "Myocybernetic Control Models of Skeletal Muscles", Biological Cybernetics, vol. 25, pp. 103-119, 1977.
9. Ogihara N and Yamazaki N, "Generation of Human Bipedal Locomotion by a Bio-mimetic Neuro-musculo-skeletal Model". Biological Cybernetics, vol. 84, pp. 1-11, 2001.
10. Kuo P and Deshpahde AD, "Contribution of Passive Properties of Muscle-tendon Units to the Metacarpophalangeal Joint Torque of the Index Finger", Proceedings of the 2010 IEEE RAS&EMBS International Conference on Biomedical Robotics and Biomechatronics (BioRob2010), pp. 288-194, 2010.
11. Riener R and Fuhr T . "Patient-Driven Control of FES-Supported Standing Up, A Simulation Study". IEEE Transactions on Rehabilitation Engineering, vol. 6, pp. 113124, 1998.
12. Schenkman M, Berger, RA, Patrick OR, Mann RW, and Hodge WA, "Whole-body Movements during Rising to Standing from Sitting", Physical Therapy, vol. 70, pp. 638-651, 1990.
13. Arnold EM, Ward SR, Lieber RL, and Delp SL, "A Model of the Lower Limb for Analysis of Human Movement", Annals of Biomedical Engineering, vol. 38, pp. 269-279, 2010.
14. Jorgensen MJ, Marras WS, Granata KP, Wian JW, "MRI-derived Moment-arms of the Female and Male Spine Loading Muscles", Clinical Biomechanics, vol. 16, pp. 182-193, 2001.